Cinchona-based zwitterionic stationary phases: Exploring retention and enantioseparation mechanisms in supercritical fluid chromatography with a fragmentation approach

Adrien Raimbault, Cam Mai Anh Ma, Martina Ferri, Stefanie Bäurer, Pascal Bonnet, Stéphane Bourg, Michael Lämmerhofer, Caroline West

Cinchona-based zwitterionic stationary phases: Exploring retention and enantioseparation mechanisms in supercritical fluid chromatography with a fragmentation approach

Adrien Raimbault[1], Cam Mai Anh Ma[1], Martina Ferri[2,3], Stefanie Bäurer[2], Pascal Bonnet[1], Stéphane Bourg[1], Michael Lämmerhofer[2], Caroline West[1]*

1. University of Orleans, Institute of Organic and Analytical Chemistry, CNRS UMR 7311, Rue de Chartres BP 6759, 45067 Orleans, France
2. Institute of Pharmaceutical Sciences, Pharmaceutical (Bio-)Analysis, University of Tübingen, Auf der Morgenstelle 8, 72076 Tübingen, Germany
3. Department of Pharmaceutical Sciences, University of Perugia, Via del Liceo 1, 06123 Perugia, Italy

caroline.west@univ-orleans.fr
tel: +33 (0) 238 49 47 78
ORCID: 0000-0001-7595-6777

Abstract

Chiralpak ZWIX(+) and ZWIX(-), are brush-type bonded-silica chiral stationary phases (CSPs), based on complex diastereomeric *Cinchona* alkaloids derivatives bearing both a positive and a negative charge. In the present study, we aimed to improve the understanding of retention and enantioseparation mechanisms of these CSPs employed in supercritical fluid chromatography (SFC). For this purpose, 9 other stationary phases were used as comparison systems: two of them are commercially available and bear only a positive charge (Chiralpak QN-AX and QD-AX) and the 7 others were designed purposely to be structurally similar to the parent ZWIX phases, but miss some portion of the complex ligand. First, cluster analysis was employed to identify similar and dissimilar behavior among the 11 stationary phases, where ionic interactions appeared to dominate the observed differences. Secondly, the stationary phases were characterized with linear solvation energy relationships (LSER) based on the SFC analysis of 161 achiral analytes and a modified version of the solvation parameter model to include ionic interactions. This served to compare the interaction capabilities for the 11 stationary phases and showed in particular the contribution of

attractive and repulsive ionic interactions. Then the ZWIX phases were characterized for their enantioseparation capabilities with a set of 58 racemic probes. Discriminant analysis was applied to explore the molecular structural features that are useful to successful enantioseparation on the ZWIX phases. In particular, it appeared that the presence of positive charges in the analyte is causing increased retention but is not necessarily a favorable feature to enantiorecognition. On the opposite, the presence of negative charges in the analyte favors early elution and enantiorecognition. Finally, a smaller set of 30 pairs of enantiomers, selected by their structural diversity and different enantioseparation values on the ZWIX phases, were analyzed on all chiral phases to observe the contribution of each structural fragment of the chiral ligand on enantioselectivity. Molecular modelling of the ligands also helped in understanding the three-dimensional arrangement of each ligand, notably the intra-molecular hydrogen bonding or the possible contribution of ionic interactions. In the end, each structural element in the ZWIX phases appeared to be a significant contributor to successful enantioresolution, whether they contribute as direct interaction groups (ion-exchange functions) or as steric constraints to orientate the interacting groups towards the analytes.

Keywords: Chiral stationary phases; Cinchona-based chiral zwitterionic ion exchanger; Enantioseparation mechanisms; Quantitative structure-retention relationships (QSRR); Solvation parameter model; Supercritical fluid chromatography

1. Introduction

Cinchona-based chiral stationary phases were introduced in the late 1980s in form of free quinine bonded to silica [1] and as carbamate derivatives in 1996 by Lämmerhofer and Lindner [2]. They are brush-type enantioselective stationary phases where the ligand is derived from quinine and quinidine diastereomers bonded on silica gel. Recently, similar phases bonded so superficially porous silica were proposed by Armstrong and co-workers [3]. Because quinine and quinidine both possess a tertiary amine function (quinuclidine ring), which should be protonated in most liquid and supercritical fluid mobile phases, a quinine- or quinidine-based stationary phase should act as an anion-exchanger. One such phase is presented in Figure 1 (**QN**). Two commercial stationary phases are available, which were derived from quinine- and quinidine-bonded silica, with a carbamate function modifying the hydroxyl group and retaining the anion-exchange capabilities: Chiralpak **QN-AX** and **QD-AX** (Figure 1). These stationary phases are mostly employed in HPLC, where they have demonstrated excellent enantioselective properties for a broad range of chiral acids [2,4]. Further modification of the carbamate function to include a chiral sulfonic acid group yielded two zwitterionic stationary phases, commercially available as Chiralpak **ZWIX(+)** and **ZWIX(-)** [5,6]. These phases were notably demonstrated to be particularly useful for the enantioseparation of free or derivatized amino acids and oligopeptides by HPLC [6–13]. Cinchona alkaloids and their derivatives were also employed as chiral selectors in capillary electrophoresis [14,15] and capillary electrochromatography [16,17], where the high efficiency values usually yield excellent resolution.

Supercritical fluid chromatography (SFC) is known to be most effective for enantioselective separations [18,19], as the resolution per unit time is often advantageous compared to HPLC separations, making it suitable for high-throughput enantioselective analysis. In addition, the economic and ecological aspects related to the use of pressurized carbon dioxide as principal component of the mobile phase render it an attractive method for the industry, both at the analytical and preparative scales. The *Cinchona*-based chiral phases were only rarely employed in SFC. One possible reason is the wrong perception that ionic species cannot exist in the apparently non-polar SFC mobile phase. However, it was proven in several studies that ionic species exist in carbon dioxide – organic solvent mixtures and can even be resolved [20,21] and that ionic interactions exist, which are measurable [4,22,23] and can be modified when acidic and basic additives are introduced in the co-solvent [24]. Thus a few papers relate the use of **ZWIX** phases to resolve N-protected amino acids [25,26] or indole-type analytes [27]. Recently, we have demonstrated that elution and enantioresolution of a

wide range of free natural amino acids were possible with a wide elution gradient running from SFC to HPLC conditions [28].

Retention and enantioseparation mechanisms on the **ZWIX** phases were explored mostly in liquid phase by the group of Lindner on the one hand [9,29], Ilisz and Péter on the other hand [30], but only little was done in SFC conditions. Pell and Lindner showed that the ion-exchange mechanism existed on **QN-AX** and **QD-AX** phases in SFC conditions, thanks to the presence of methoxylcarbonic acid formed by the reaction of CO_2 and acting as counterion in the anion-exchange process [4]. This ion-exchange mechanism could be tuned with the introduction of acidic or basic additives in the mobile phase. For these stationary phases, the same chiral recognition mechanism was observed between HPLC and SFC experiments. More recently, Wolrab *et al*. observed major differences between HPLC and SFC separations on the **ZWIX** phases and proceeded to explain the differences [31]. A major conclusion from this work is that mechanistic investigations done on the **ZWIX** phases in HPLC conditions may not all be transferable to SFC conditions. Naturally, the components of the mobile phase can have a significant contribution to the enantiorecognition as they define the environment in which the process occurs [6,30,32], may have different solvation properties towards the chiral analytes and the chiral stationary phase, which is sometimes resulting in different conformations of the stationary phase.

To better understand the behavior of Chiralpak **ZWIX(+)** and **ZWIX(-)** in SFC, a fragment-based approach to deciphering the complex enantioselective ligands was selected: nine other (commercial or in-house) stationary phases were used as comparison. All nine phases had some similarity to the **ZWIX** phases, each one having one less fragment than the parent ligand. The purpose was to understand the contribution of each functional group in the retention mechanisms and appreciate how each functional group was determinant in the enantioseparation process. For this purpose, the eleven columns were first characterized by means of quantitative structure-retention relationships (QSRR) with a modified version of the solvation parameter model, to include ionic interactions, based on the analysis of 161 achiral analytes. Cluster analysis and the QSRR models served to compare the columns. Secondly, based on the analysis of 58 racemic probes, discriminant analysis served to identify the molecular features that are most favorable to successful enantioseparation on the ZWIX phases. Finally, 30 racemates with structural diversity were analyzed to explore the differences in enantioresolution. Molecular modelling assisted in understanding the observed differences.

2. Material and methods

2.1 Stationary phases

All experiments were carried out on the eleven columns. Four columns are commercially available, named Chiralpak **ZWIX(+)**, Chiralpak **ZWIX(-)**, Chiralpak **QN-AX** and Chiralpak **QD-AX**, and were kindly provided by Chiral Technologies Europe (Illkirch, France) with ligands bonded on 3 µm particles. The seven other ligands were prepared in-house, bonded on 3 µm Daisogel silica, 120 Å (Osaka Soda) and packed. Their synthesis and liquid-phase characterization was described in a previous study [33]. All columns had the same dimensions of 150 x 3 mm.

2.2 Chemicals and Solvents

161 achiral (Table S1) and 66 chiral molecules (Table S2) in their racemic form were purchased from Sigma-Aldrich (Sigma Aldrich Chimie, France). The achiral analytes were selected to provide a diverse representation of chemical functions to obtain meaningful retention models with the solvation parameter model. The chiral probes in Table S2 were selected to obtain meaningful information from the discriminant analyses with different structures and shapes. These sets were fully described in previous papers [34,35]. The reduced set of chiral analytes (Table S2, in bold) was selected as a subset of the wider set maintaining structural diversity but also included an addition of 8 free amino acids. As the individual enantiomers were not available in most cases, the elution order was not assessed. Solutions of all analytes were prepared at about 1 mg/mL in methanol (MeOH). The HPLC-grade methanol used for analyte dissolution and as mobile phase co-solvent was supplied by VWR (Fontenay-sous-Bois, France). Ultra-pure water was supplied by an Elga UHQ system from Veolia (Wissous, France). CO_2, with a purity of 99.995 %, was delivered by Air Liquide (Paris, France). Ammonium formate was provided by Sigma Aldrich (Sigma Aldrich Chimie, France).

2.3 Instruments and operating conditions

The supercritical fluid chromatography system was an ACQUITY Ultra Performance Convergence Chromatography™ (UPC$^{2®}$) from Waters Corporation (Millford, MA, USA). It was equipped with a binary solvent delivery pump compatible with mobile phase flow rates up to 4 mL/min and pressures up to 414 bar, an autosampler that included partial loop volume injection system, a back-pressure regulator, 2-position column oven compatible with 150 mm length columns and a photodiode-array (PDA) detector. Empower® 3 was used for integration of peaks for column efficiency measurements. An ACQUITY QDa® single-quadrupole mass detector with electrospray ionization source was also used for amino acids

detection. An isocratic solvent manager was used as a make-up pump and was positioned before the mass detector. The main flow stream was then split by the on-board flow-splitter assembly.

All analyses (chiral and achiral sets) were performed in isocratic conditions (CO_2-MeOH 90:10 (v/v), 25°C, 150 bar, 3 mL/min), apart from the analyses of amino acids for which a wide gradient elution (10 to 100% co-solvent) was done with methanol containing 5% H_2O and 50 mM ammonium formate, according to previously developed method [28]. In that, case, the flow rate was reduced to 0.5 mL/min to avoid reaching the upper pressure limit of the pumping system. The UV detection wavelength was 210 nm while single-ion recording was used for MS detection of amino acids according to the mass of the protonated molecular ion.

2.4 Data analysis

Abraham descriptors (Tables S1 and S2) were extracted from an in-house database based on all existing literature on the solvation parameter model. Additional structural descriptors were computed as previously described [22,35].

Multivariate data analyses (hierarchical cluster analysis (HCA), multiple linear regression and discriminant analysis (DA)) were done with XLSTAT 19.03 software (Addinsoft, New York, NY, USA). The retention data (log *k* values) for achiral analytes were normalized (centred and reduced to adjust mean value on 0 and standard deviation on 1) prior to HCA calculation, to ensure that equal significance would be associated to each analyte. HCA was based on Ward aggregation method with Euclidean distance.

The quality of QSRR fits was estimated using the adjusted determination coefficient (R^2_{adj}), standard error in the estimate (*SE*) and Fisher *F* statistic. The statistical significance of individual coefficients was evaluated with the 95% confidence intervals.

The linear solvation energy relationship (LSER) equation used in this work is based on the five Abraham descriptors and two additional descriptors to take ionic interactions into account:

$$\log k = c + eE + sS + aA + bB + vV + d^-D^- + d^+D^+ \quad (1)$$

In this equation, capital letters represent the solute descriptors, related to particular interaction properties, each molecule has its own molecular descriptors. While lower case letters represent the system constants, related to the complementary effect of the two phases (stationary and mobile). *c* is the model intercept term and is dominated by the phase

ratio. *E* is the excess molar refraction (calculated from the refractive index of the molecule) and models polarizability contributions from *n* and *π* electrons; *S* quantifies the presence of dipoles and polarizability; *A* and *B* are the solute overall hydrogen-bond acidity and basicity; *V* is the McGowan characteristic volume in units of $cm^3\ mol^{-1}/100$; D^- and D^+ are the solute negative and positive charges respectively, calculated with the pK_a and apparent pH of the mobile phase. The five first descriptors are known as Abraham descriptors and were used in many occasions to characterize chromatographic systems, while the latter two were introduced more recently to characterize hydrophilic interaction liquid chromatography (HILIC) systems [36], and were later demonstrated to be suitable to describe SFC systems, provided we admit to some approximations [22,23]. The system constants (*e*, *s*, *a*, *b*, *v*, d^-, d^+), obtained through a multilinear regression of the retention data for a certain number of solutes with known descriptors, reflect the magnitude of difference for that particular property between the mobile and stationary phases. Thus, if a particular coefficient is numerically large, then any solute having the complementary property will interact very strongly with either the mobile phase (if the coefficient is negative) or the stationary phase (if the coefficient is positive). The system constants facilitate the comparison of the separation characteristics of different stationary phases and enable the identification of stationary phases of similar or dissimilar selectivity.

In previous works, we have demonstrated that two other structural features that contributed little to retention were however significant to describe enantioseparation mechanisms on polysaccharide or macrocylic glycopeptide stationary phases: flexibility (F) and globularity or sphericity (G) [35,37–39]. In the present work, the F and G descriptors were first introduced in Equation (1) but appeared to be insignificant to explain retention. They were however retained for the evaluation of chiral separations through discriminant analysis. The quality of discriminant analysis was estimated based on ROC (receiver operating characteristics) curves (visible in Figure S1) and confusion matrices.

2.5 Molecular modelling

The 3D structures of each enantioselective ligand presented in Figure 1 were prepared from 2D coordinates. The 3D conformations were generated using the Structure Preparation function and hydrogen atoms were added using Protonate3D function in MOE2014.09 (Chemical Computing Group Inc., Montreal, Canada). Then the structures were submitted to conformational search using LowModeMD with default parameters. The MMFF94x force field with Born solvation was used and the lowest energy conformer was retained for comparison of the ligand conformations. The structures were observed and copied from Discovery Studio 4.0 Visualizer (Accelery, San Diego, California, USA).

3. Results and discussion

3.1 Description of the stationary phases

The chiral selectors in the eleven stationary phases compared in this study are presented in Figure 1.

As can be seen in Figure 1, apart from the above-cited **ZWIX(+)**, **ZWIX(-)**, **QN**, **QN-AX** and **QD-AX**, six other fragmented ligands were designed. First, removal of the quinoline group from the **ZWIX(+)** and **ZWIX(-)** chiral selectors yielded **QCISS** and **QCDRR** ligands, respectively. The steric constriction of the sulfonic group was further removed to yield **QCITAU** and **QCDTAU**, based on quincorine (QCI) / quincoridine (QCD) and taurine (TAU). Finally, the cationic quincoridine group was removed from **QCDRR** and **QCDTAU** to obtain the strong cation-exchangers 2-aminocyclohexanesulfonic acid-derived **SCXSS** and taurine-derived **SCXTAU**. The ligand coverage on the stationary phase surface was adjusted to ca. 200 µmol/g (within ± 30 µmol/g) for all stationary phases [33].

All these phases (the seven in-house and the Chiralpak **QN-AX** and **QD-AX**) were highly similar to the **ZWIX** phases, each one having only some portion of the structure less than the original ligand. The purpose was to understand the involvement of each functional group in the retention and enantioseparation mechanisms and measure how each functional group was determinant in the enantioseparation process. Due to the large number of stationary phases and the number of analytes included to obtain most accurate and representative models, only one mobile phase composition was employed, although acidic and basic additives should clearly have an effect on enantioselective capabilities of these phases [31].

3.2 Multivariate data analysis: Hierarchical cluster analysis

Hierarchical cluster analysis (HCA) is a useful method to group chromatographic columns according to the similarity in their retention behaviour. Because the retention data were normalized, the similarity will reflect elution order of the analytes, rather than overall retention. The result are presented in a dendrogram (Figure 2), where the columns that are linked with a short horizontal line are most similar and have close chromatographic selectivity, and the columns that are linked with a long horizontal line are most dissimilar and exhibit different chromatographic selectivity. In Figure 2, three principal clusters appear:

- In the upper part of the figure, the **ZWIX(+)** and **ZWIX(-)** phases are grouped with the four other zwitterionic phases **QCITAU**, **QCISS**, **QCDRR** and **QCDTAU**.
- In the middle of the figure, the three phases possessing only a cationic charge are grouped (**QN**, **QN-AX** and **QD-AX**).
- In the lower part of the figure, the two phases possessing only an anionic charge are grouped (**SCXSS** and **SCXTAU**).

Clearly, the clustering is mostly based on ionic interactions, while the presence of quinoline and the hexyl ring on the sulfonic group are much less significant in terms of retention behaviour. Quite logically, diastereomeric or pseudoenantiomeric phases are most similar (linked with the smallest lines): **ZWIX(+)** and **ZWIX(-)**; **QN-AX** and **QD-AX**; **QCISS** and **QCDRR**; **QCITAU** and **QCDTAU**.

While the dendrogram is a simple way to compare columns, it is not highly informative. Therefore, linear solvation energy relationships were calculated for each column to explore interaction differences more precisely.

3.3 Retention mechanisms examined with achiral compounds

161 achiral molecules (Table S1) were analyzed on the eleven columns studied in order to model their retentive properties. A modified version of the LSER model (Equation (1)) was used with the five Abraham descriptors and the addition of two descriptors taking ionic interactions into account. The model therefore contains a total of seven different descriptors. The results are presented in Table 1 and Figure 3. Considering that no retention prediction was desired (only interpretation of interaction terms), the statistics were considered as reasonably good.

Retention mechanisms on all eleven phases are dominated by hydrogen bonding with proton donors (*a* terms) and by interactions with π and n electrons (*e*) that must result principally from π-stacking with aromatic analytes. Hydrogen-bonding with proton acceptors (*b* term), the contribution of molecular volume (*v*) and ionic interactions (d^- and d^+ terms) are significant on certain columns and are clearly discriminant. Dipole-dipole interactions (*s*) contribute moderately and offer little discrimination between the stationary phases examined.

Examining the models obtained on the **ZWIX** phases, a first, quite surprising observation is that the ionic interaction terms (d^- and d^+) are rather small although significant ionic interactions were expected. The d^+ term is slightly larger than the d^- term, in accordance with previous reports that the surface of **ZWIX** stationary phases is slightly acidic [40]. Besides, the four other zwitterionic phases (**QCISS**, **QCDRR**, **QCITAU** and **QCDTAU**) also have

rather small ionic interaction terms. This would tend to indicate that the cationic and anionic groups in the ligands must be associated to each other, thereby reducing their availability for interaction with ionic analytes. Indeed, the d^- term, reflecting retention of anionic compounds, is large and positive on the anion-exchange stationary phases (**QN-AX**, **QD-AX** and **QN**) while the d^+ term, reflecting retention of cationic compounds, is large and positive on the cation-exchange stationary phases (**SCXSS** and **SCXTAU**). In addition, the d^+ term, reflecting retention of cationic compounds, is reduced on the anion-exchange stationary phases while the d^- term, reflecting retention of anionic compounds, is large and negative on the cation-exchange stationary phases, probably due to electrostatic repulsion interactions. In the case of simple ion-exchangers (not zwitterionic), the charges on the ligands are thus more freely available to interact with ionic analytes than on the **ZWIX** phases. On the contrary, the phases possessing a single ionic function, whether it is cationic or anionic, display strong ionic interactions. This is consistent with previous observations in HPLC that the sulfonic group "mostly act as intramolecular counterions leading to reduced run times compared to parent anion exchangers" [5]. Another interesting explanation for the moderate values of d^- and d^+ terms may be found in the electrostatic attraction-repulsion (push-and-pull) mechanism recently proposed by Mimini *et al*. [41]. Basically any anionic analyte should be both attracted by the cationic function of the stationary phase and repulsed by the anionic function, and vice-versa for an anionic analyte. This combined effect of attraction and repulsion could explain the overall moderate retention of ionic species on the **ZWIX** phases. In other words, the two ionic functions in the chiral ligand partly cancel each other.
Another interesting feature is that the *v* term, reflecting the effect of molecular volume on retention, is negative on all stationary phases but most significant on the **ZWIX** phases. The negative terms indicate that an increase in hydrocarbon volume is causing decreased retention on all columns, as usually observed on polar stationary phases in SFC [42], related to a normal-phase retention mode. The most significant negative value of *v* term on **ZWIX** phases can be related to the difficulty for large molecules to insert in the stationary phase, due to the bulky ligand leaving little space for insertion, or due to the cohesiveness of the stationary phase resulting from ionic and hydrogen-bonding interactions between them. Only the strong cation exchanger **SCXTAU** had comparably large negative *v* term, which can be explained by the absence of hydrophobic ligand portion in this stationary phase that could contribute to positive dispersive interactions to compensate for the phase cohesiveness.

Compared to **ZWIX** phases, the four other zwitterionic columns **QCISS**, **QCDRR**, **QCITAU** and **QCDTAU** are lacking a quinoline group, and two of them are lacking a butyl linker that is constraining the sulfonic group through a cyclohexyl function.

A small increase is observed for the interactions with anionic species (d^-), and a small decrease for the interactions with cationic species (d^+) for the phases that do not possess a quinoline group, which may be attributed to easier access of the ionic analytes to the cationic charge borne by the protonated nitrogen atom, when the bulky quinolic group is absent, causing increased attraction of anions and increased repulsion of cations. Other terms were mostly similar on all zwitterionic phases.

The three phases **QN-AX**, **QD-AX** and **QN** are similar to the **ZWIX** phases apart from the sulfonic group. As mentioned above, the most significant differences observed are in the ionic interactions and *v* term. On a practical note, this will reflect on the retention of acidic species that should comparatively be more retained on the anion-exchange stationary phases than on the zwitterionic phases, as appears in Figure 4a. In this figure, it appears that the retention of Chiralpak **ZWIX(+)** and Chiralpak **QN-AX** are most similar, apart from the species that should bear a negative charge in the present operating conditions. Other small differences are noticeable in Figure 3: a small decrease of hydrogen bonding with proton donors and acceptors (*a* and *b* terms respectively) and interactions with dipoles and polarizable species (*s* and *e* terms respectively) are observed for the 3 phases possessing no sulfonic group when compared to the **ZWIX** phases.

The simple cation-exchangers **SCXSS** and **SCXTAU** are the most different from the ZWIX phases, not only due to a different pattern of ionic interactions, but also with significantly weaker hydrogen bonding interactions with proton donors (*a* term) and significantly stronger hydrogen bonding with proton acceptors (*b* term). Overall, this reflects in generally weaker retention on the cation-exchange phases compared to the zwitterionic phases, as appears in Figure 4b, where most points fall below the first bisector. However, when a trend line is plotted across hydrophobic analytes (black diamonds), although some dispersion appears for polar non-ionic analytes (open circles), the lower retention of acidic anionic compounds (red triangles) and the stronger retention of basic cationic analytes (blue squares) are evident.

Finally, based on the LSER models, the eleven phases were plotted in the spider diagram reflecting the overall selectivity of the phases (Figure 5). This figure was previously developed to allow easy comparison of a large number of stationary phases based on the system constants from LSER characterization [23,43]. Quite simply, the figure is a projection of the seven-dimension selectivity space defined by the seven system constants in Eq. (1) on a plane. Most hydrophobic stationary phases are situated on the left of the figure and most polar stationary phases are located on the right. From top to bottom, hydrogen bonding and ionic interactions contribute significantly to scattering the stationary phases. Bubble size is related to the overall strength of interactions (length of the solvation vector). To better appreciate the diversity of selectivities provided by the eleven phases, 36 other stationary

phases previously characterized with the same protocol were also plotted. The full list of the columns relating to their number in the figure is presented in Table S3.

A first observation is that all eleven phases are grouped on the right of the figure, with polar stationary phases, but they are clearly scattered along the vertical axis, as a result of their different ionic interactions: the anion-exchange stationary phases are grouped at the bottom of the figure, the cation-exchange phases are situated in the upper part of the figure, and the zwitterionic phases are in-between. Secondly, all eleven phases are singular (not superimposed with any other in the figure) but have some similarity to other phases. The **ZWIX** phases are not too far from the achiral zwitterionic phases based on sulfobetaine ligand (# 22 and 23). They are also close to a stationary phase bonded with amino-anthracene ligand, probably due to the similarity to the quinoline group. The cation-exchange phases are not too far from the bare silica phases (# 31-36) which can also interact with cationic analytes through their silanol groups. Finally, the phases possessing amine or pyridine groups in their bonded ligands (# 21, 24 and 25) are all at the bottom of the figure, close to the zwitterionic and anion-exchange phases characterized in this work.

3.4 Enantioseparation mechanism examined with discriminant analysis

In previous studies on polysaccharide or macrocyclic glycopeptide enantioselective stationary phases, we have demonstrated that discriminant analysis was a useful tool to understand the molecular features that contribute to favorable enantiorecognition [37–39]. Basically, discriminant analysis is applied to a diverse selection of racemates (58 in the present case) analyzed in a single chromatographic system (one stationary phase and one mobile phase composition). The probe molecules are characterized by molecular descriptors and by the chromatographic result that can be simplified in two categories: separated (separation factor > 1) or not separated (separation factor = 1). However, we had also observed that applying this strategy to the whole set of racemates was often unsuccessful because not all racemates that were resolved had been discriminated for the same reasons. Thus a discriminant analysis including the whole set of analytes usually results in poor statistics, indicating that the models obtained are not relevant. To improve the significance of the results, a more efficient strategy was defined. First, the experimental retention of the two enantiomers is compared to the theoretical retention predicted with the solvation parameter model (Eq. (1)). In most cases, the two enantiomers both elute earlier than the prediction or they both elute later than the prediction. A first discriminant analysis is then carried out to observe the features that contribute to early elution or late elution of the enantiomers. At this

stage, it is useful to introduce two additional descriptors that are helpful to describe enantiorecognition processes: flexibility (F) and globularity (G). The other descriptors are the same seven used in the LSER models above.

The result of this discriminant analysis can be observed for Chiralpak **ZWIX(-)** in Figure 6a. It appears that late-eluting analytes are mostly flexible molecules (positive F term) and cationic molecules (positive D^+ term). Flexible molecules have more ways to adapt to a complex, rather rigid ligand, which should be favorable to increased possibilities of interactions between a multi-functional analyte and the multi-functional ligand. The favorable contribution of positive charges may be related to better accessibility of the anionic sulfonic group than the cationic quinuclidine causing stronger retention for cations. Conversely, anionic compounds seem to be repulsed as the presence of negative charges is favorable to early elution (negative D^- term). This may be observed on a molecular model of the Chiralpak **ZWIX(-)** ligand in Figure 7, where the quinuclidine group, being closer to the silica surface, should be most difficult to interact with than the pending sulfonic group.

Secondly, discriminant analysis based on the separated / non separated classes is applied independently on the 32 early-eluting (Figure 6b) and 26 late-eluting racemates (Figure 6c). Comparing the two figures, it appears that the structural features that contribute favorably to enantiorecognition are not all identical between early-eluting and late-eluting racemates. More precisely, the same three features (acidic character A, globularity G and negative charges D^-) appear to be favorable but not in the same proportions. For early-eluting analytes, which should be rather rigid and not cationic, the presence of a negative charge is the most favorable feature (large positive D^- term), followed by proton-donor capability (positive A term). We may suppose that the ability to interact favorably with the cationic group (quinuclidine function) and with the quinoline and/or carbamate functions must contribute favorably to enantiorecognition. Late-eluting molecules are mostly cationic and flexible, but these features are not favorable to enantiorecognition for this group (negative F and D^+ terms).

In both cases (early and late-eluting), globularity is highly significant (positive G term) while small molecular volume is also a favorable feature (negative V term). This indicates that small spherical molecules are generally better resolved with this chiral selector. The chiral selector is rather constrained with three rather rigid portions: the quinoline ring, the quinuclidine group and the cyclohexanesulfonic function. The three of them define a small space for chiral molecules to fit in. A small spherical molecule should better adapt to this defined space than a large and/or non-spherical (planar or linear) molecule.

Very similar results were obtained in all cases on Chiralpak **ZWIX(+)**.

A subset of the 58 racemates was selected for structural diversity: 22 molecules (written in bold in Table S2) representing different analyte classes and with different separation features on the **ZWIX** phases (resolved or nor resolved) were chosen. Additionally, 8 free amino acids that were resolved on the **ZWIX** phases were included in this final test set. The 30 pairs of enantiomers were analysed on the ten chiral phases (thus excluding the non-chiral **SCXTAU**). Some representative examples are shown in Table 2. Only racemates that could be resolved on one stationary phase at least are presented in this table because the racemates that cannot be (at least partially) resolved on any stationary phase provide little information on enantiorecognition mechanisms.

One example of the contribution of shape is that of benzodiazepines. For instance, Oxazepam is a large and rather flat molecule. Because of its rigidness, it was eluted rather earlier than predicted but its flatness is probably responsible for the lack of enantioresolution on the **ZWIX** phases. Some enantioselectivity was however observed on the **QN-AX** and **QD-AX** phases. Molecular modelling allows observing the different three-dimensional orientation of each CSP ligand: the folding of each ligand is highly dependent on intra-molecular interactions and steric constraints. Comparing the structures of the ligands (see superimposed ligands of **ZWIX(-)** and **QD-AX** in Figure 7), it appears that the structure of **QN-AX** and **QD-AX** should be more open, less sterically constrained than the structure of **ZWIX** ligands. The replacement of the large cyclohexylsulfonic group by a smaller t-butyl group should make it easier for a large molecule to adapt to the chiral selector.

On the contrary, 5-methyl-5-phenylhydantoin is a small and rather compact (spherical) molecule that was well resolved on the **ZWIX** phases, as can be seen in the chromatograms in Figure 8a. Resolution was also possible on the anion-exchange phases (**QN-AX**, **QD-AX** and **QN**), and it was also possible on the two phases lacking the quinoline group but retaining the cyclohexyl group (**QCISS** and **QCDRR**). However, enantioseparation was lost when the steric constraint on the sulfonic group was not present (**QCITAU** and **QCDTAU**). Clearly, the orientation of the sulfonic group, forced by the presence of the cyclohexyl group, is favorable to enantiorecognition. This observation can be contrasted to previous observations in the liquid phase that "the *trans*-2-aminocyclohexanesulfonic acid moiety… is truly beneficial but not essential for the observed enantioselective properties of the zwitterionic chiral stationary phases" [5].

Acidic compounds and proton-rich compounds were generally well resolved on **ZWIX** phases and anion exchangers, while no resolution could be obtained on the other columns. Only the anion-exchange phases were also favorable to resolution of acids.

Enantiorecognition was observed for all amino acids on the **ZWIX** phases as a result of the double ion-pairing with the zwitterionic analytes [30] but was lost on most of the others, apart from the other zwitterionic phases where some enantioselectivity may be observed, even if the peak shapes were poor. An example can be seen in Figure 8b with the chromatograms of Alanine. The zwitterionic character thus seems necessary but not sufficient to ensure enantioresolution of zwitterionic analytes. Comparing the ligand structures in Figure 7, the **QCISS** ligand should be much more flexible than the **ZWIX(+)** ligand as the large quinoline group is not present to force the conformation in one direction. Flexibility in a chiral selector is generally recognized as an unfavorable feature.

The simplest ligand in **SCXSS** was totally incapable of resolving any of the pairs of enantiomers in this set. Clearly, the simple chirality borne by the cyclohexylsulfonic ligand is not sufficient to discriminate the enantiomers.

Overall, among the 22 pairs of enantiomers other than amino acids, 7 are separated on the **ZWIX** phases, whereas 8 pairs of enantiomers were separated on the **QN-AX** and **QD-AX** phases, 6 pairs on the **QN** phase and only 2 on the four other zwitterionic phases.

All structural features in the **ZWIX** phases then seem to play a significant role in the multi-modal enantioseparation mechanism. This synergistic effect that was desired in the conception of the **ZWIX** ligands [5] is then proven to be completely true.

4. Conclusion

The mechanisms for retention and enantioseparation of the Chiralpak ZWIX(+/-) columns were studied with the analysis of 161 achiral compounds and 66 pairs of enantiomers. The joint presence of a cationic and anionic charge in the **ZWIX** phases appears to be reducing the overall strength of ionic interactions, compared to simple anion-exchange or cation-exchange phases, probably due to intra-molecular ionic interactions, or ionic interactions between proximate ligands. The influence of the sterically constrained sulfonic group and the quinoline group were shown to be highly significant to explain the successful enantiorecognition in the **ZWIX** phases. Basically, all structural elements of the **ZWIX** ligands appeared to be significant contributors to enantioselectivity. **ZWIX** phases also appeared to favour small and spherical molecules, which should better fit in the chiral selector cavity, as large and/or flat molecules remained unresolved.

Acknowledgments

Adrien Raimbault is grateful for a PhD grant received from the Ministry of Higher Education and Research. Caroline West is grateful for the support received by the Institut Universitaire de France (IUF), of which she is a Junior Member. Pilar Franco (Chiral Technologies Europe) is warmly acknowledged for the gift of columns and for interesting discussions.

Compliance with ethical standards

The authors declare they have no conflict of interest.

[1] C. Rosini, C. Bertucci, D. Pini, P. Altemura, P. Salvadori, Cinchona alkaloids for preparing new, easily accessible chiral stationary phases.I. 11-(10,11-Dihydro-6'-methoxy-cinchonan-9-OL)-tiopropylsilanized silica., Tetrahedron Lett. 26 (1985) 3361–3364. https://doi.org/10.1016/S0040-4039(00)98298-4.
[2] M. Lämmerhofer, W. Lindner, Quinine and quinidine derivatives as chiral selectors I. Brush type chiral stationary phases for high-performance liquid chromatography based on cinchonan carbamates and their application as chiral anion exchangers, J. Chromatogr. A. 741 (1996) 33–48. https://doi.org/10.1016/0021-9673(96)00137-9.
[3] D.C. Patel, Z.S. Breitbach, J. Yu, K.A. Nguyen, D.W. Armstrong, Quinine bonded to superficially porous particles for high-efficiency and ultrafast liquid and supercritical fluid chromatography, Anal. Chim. Acta. 963 (2017) 164–174. https://doi.org/10.1016/j.aca.2017.02.005.
[4] R. Pell, W. Lindner, Potential of chiral anion-exchangers operated in various subcritical fluid chromatography modes for resolution of chiral acids, J. Chromatogr. A. 1245 (2012) 175–182. https://doi.org/10.1016/j.chroma.2012.05.023.
[5] C.V. Hoffmann, R. Pell, M. Lämmerhofer, W. Lindner, Synergistic Effects on Enantioselectivity of Zwitterionic Chiral Stationary Phases for Separations of Chiral Acids, Bases, and Amino Acids by HPLC, Anal. Chem. 80 (2008) 8780–8789. https://doi.org/10.1021/ac801384f.
[6] T. Zhang, E. Holder, P. Franco, W. Lindner, Zwitterionic chiral stationary phases based on cinchona and chiral sulfonic acids for the direct stereoselective separation of amino acids and other amphoteric compounds: Liquid Chromatography, J. Sep. Sci. 37 (2014) 1237–1247. https://doi.org/10.1002/jssc.201400149.
[7] Z. Pataj, I. Ilisz, Z. Gecse, Z. Szakonyi, F. Fülöp, W. Lindner, A. Péter, Effect of mobile phase composition on the liquid chromatographic enantioseparation of bulky monoterpene-based β-amino acids by applying chiral stationary phases based on *Cinchona* alkaloid: Liquid Chromatography, J. Sep. Sci. 37 (2014) 1075–1082. https://doi.org/10.1002/jssc.201400078.
[8] S. Wernisch, W. Lindner, Versatility of cinchona-based zwitterionic chiral stationary phases: Enantiomer and diastereomer separations of non-protected oligopeptides utilizing a multi-modal chiral recognition mechanism, J. Chromatogr. A. 1269 (2012) 297–307. https://doi.org/10.1016/j.chroma.2012.06.094.
[9] N.M. Maier, S. Schefzick, G.M. Lombardo, M. Feliz, K. Rissanen, W. Lindner, K.B. Lipkowitz, Elucidation of the Chiral Recognition Mechanism of Cinchona Alkaloid Carbamate-type Receptors for 3,5-Dinitrobenzoyl Amino Acids, J. Am. Chem. Soc. 124 (2002) 8611–8629. https://doi.org/10.1021/ja020203i.
[10] T. Zhang, E. Holder, P. Franco, W. Lindner, Method development and optimization on cinchona and chiral sulfonic acid–based zwitterionic stationary phases for enantiomer separations of free amino acids by high-performance liquid chromatography, Enantioseparations - 2014. 1363 (2014) 191–199. https://doi.org/10.1016/j.chroma.2014.06.012.
[11] T. Fukushima, A. Sugiura, I. Furuta, S. Iwasa, H. Iizuka, H. Ichiba, M. Onozato, H. Hikawa, Y. Yokoyama, Enantiomeric Separation of Monosubstituted Tryptophan Derivatives and Metabolites by HPLC with a *Cinchona* Alkaloid-Based Zwitterionic Chiral Stationary Phase and Its Application to the Evaluation of the Optical Purity of Synthesized 6-Chloro-L-Tryptophan, Int. J. Tryptophan Res. 8 (2015) IJTR.S20381. https://doi.org/10.4137/IJTR.S20381.
[12] I. Ilisz, Z. Gecse, G. Lajkó, E. Forró, F. Fülöp, W. Lindner, A. Péter, High-Performance Liquid Chromatographic Enantioseparation of Cyclic *β* -Amino Acids on Zwitterionic Chiral Stationary Phases Based on *Cinchona* Alkaloids: HPLC Enantioseparation of Cyclic *β* -Amino Acids, Chirality. 27 (2015) 563–570. https://doi.org/10.1002/chir.22458.
[13] I. Ilisz, N. Grecsó, R. Papoušek, Z. Pataj, P. Barták, L. Lázár, F. Fülöp, W. Lindner, A. Péter, High-performance liquid chromatographic separation of unusual β3-amino acid enantiomers in different chromatographic modes on Cinchona alkaloid-based zwitterionic chiral stationary phases, Amino Acids. 47 (2015) 2279–2291. https://doi.org/10.1007/s00726-015-2006-1.

[14] M. Lämmerhofer, E. Zarbl, W. Lindner, tert.-Butylcarbamoylquinine as chiral ion-pair agent in non-aqueous enantioselective capillary electrophoresis applying the partial filling technique, J. Chromatogr. A. 892 (2000) 509–521. https://doi.org/10.1016/S0021-9673(00)00172-2.
[15] A.M. Stalcup, K.H. Gahm, Quinine as a chiral additive in nonaqueous capillary zone electrophoresis, J. Microcolumn Sep. 8 (1996) 145–150. https://doi.org/10.1002/(SICI)1520-667X(1996)8:2<145::AID-MCS8>3.0.CO;2-1.
[16] M. Lämmerhofer, E. Tobler, E. Zarbl, W. Lindner, F. Svec, J.M.J. Fréchet, Macroporous monolithic chiral stationary phases for capillary electrochromatography: New chiral monomer derived from cinchona alkaloid with enhanced enantioselectivity, ELECTROPHORESIS. 24 (2003) 2986–2999. https://doi.org/10.1002/elps.200305527.
[17] M. Lämmerhofer, F. Svec, J.M.J. Fréchet, W. Lindner, Chiral Monolithic Columns for Enantioselective Capillary Electrochromatography Prepared by Copolymerization of a Monomer with Quinidine Functionality. 2. Effect of Chromatographic Conditions on the Chiral Separations, Anal. Chem. 72 (2000) 4623–4628. https://doi.org/10.1021/ac000323d.
[18] C. West, Enantioselective Separations with Supercritical Fluids - Review, Curr. Anal. Chem. 10 (2014) 99–120. https://doi.org/10.2174/1573411011410010009.
[19] C. West, Recent trends in chiral supercritical fluid chromatography, TrAC Trends Anal. Chem. 120 (2019) 115648. https://doi.org/10.1016/j.trac.2019.115648.
[20] C. Foulon, P. Di Giulio, M. Lecoeur, Simultaneous determination of inorganic anions and cations by supercritical fluid chromatography using evaporative light scattering detection, J. Chromatogr. A. 1534 (2018) 139–149. https://doi.org/10.1016/j.chroma.2017.12.047.
[21] M.O. Kostenko, K.B. Ustinovich, O.I. Pokrovskiy, O.O. Parenago, N.G. Bazarnova, V.V. Lunin, Effect of the Mobile Phase Composition on Selectivity in Supercritical Fluid Chromatography in the Separation of Salbutamol Enantiomers, Russ. J. Phys. Chem. B. 12 (2018) 1166–1175. https://doi.org/10.1134/S1990793118070059.
[22] C. West, E. Lemasson, S. Khater, E. Lesellier, An attempt to estimate ionic interactions with phenyl and pentafluorophenyl stationary phases in supercritical fluid chromatography, J. Chromatogr. A. 1412 (2015) 126–138. https://doi.org/10.1016/j.chroma.2015.08.009.
[23] C. West, E. Lemasson, S. Bertin, P. Hennig, E. Lesellier, An improved classification of stationary phases for ultra-high performance supercritical fluid chromatography, J. Chromatogr. A. 1440 (2016) 212–228. https://doi.org/10.1016/j.chroma.2016.02.052.
[24] C. West, E. Lemasson, Unravelling the effects of mobile phase additives in supercritical fluid chromatography. Part II: Adsorption on the stationary phase, J. Chromatogr. A. (2019). https://doi.org/10.1016/j.chroma.2019.02.002.
[25] G. Lajkó, I. Ilisz, G. Tóth, F. Fülöp, W. Lindner, A. Péter, Application of Cinchona alkaloid-based zwitterionic chiral stationary phases in supercritical fluid chromatography for the enantioseparation of Nα-protected proteinogenic amino acids, J. Chromatogr. A. 1415 (2015) 134–145. https://doi.org/10.1016/j.chroma.2015.08.058.
[26] G. Lajkó, N. Grecsó, G. Tóth, F. Fülöp, W. Lindner, I. Ilisz, A. Péter, Liquid and subcritical fluid chromatographic enantioseparation of N^{α}-Fmoc proteinogenic amino acids on *Quinidine*-based zwitterionic and anion-exchanger type chiral stationary phases. A comparative study, Chirality. 29 (2017) 225–238. https://doi.org/10.1002/chir.22700.
[27] A. Bajtai, G. Lajkó, I. Szatmári, F. Fülöp, W. Lindner, I. Ilisz, A. Péter, Dedicated comparisons of diverse polysaccharide- and zwitterionic Cinchona alkaloid-based chiral stationary phases probed with basic and ampholytic indole analogs in liquid and subcritical fluid chromatography mode, J. Chromatogr. A. 1563 (2018) 180–190. https://doi.org/10.1016/j.chroma.2018.05.064.
[28] A. Raimbault, M. Dorebska, C. West, A chiral unified chromatography–mass spectrometry method to analyze free amino acids, Anal. Bioanal. Chem. (2019). https://doi.org/10.1007/s00216-019-01783-5.
[29] R. Pell, S. Sić, W. Lindner, Mechanistic investigations of cinchona alkaloid-based zwitterionic chiral stationary phases, J. Chromatogr. A. 1269 (2012) 287–296. https://doi.org/10.1016/j.chroma.2012.08.006.

[30] I. Ilisz, A. Bajtai, W. Lindner, A. Péter, Liquid chromatographic enantiomer separations applying chiral ion-exchangers based on Cinchona alkaloids, J. Pharm. Biomed. Anal. 159 (2018) 127–152. https://doi.org/10.1016/j.jpba.2018.06.045.
[31] D. Wolrab, P. Frühauf, C. Gerner, M. Kohout, W. Lindner, Consequences of transition from liquid chromatography to supercritical fluid chromatography on the overall performance of a chiral zwitterionic ion-exchanger, J. Chromatogr. A. 1517 (2017) 165–175. https://doi.org/10.1016/j.chroma.2017.08.022.
[32] M. Lämmerhofer, Chiral recognition by enantioselective liquid chromatography: Mechanisms and modern chiral stationary phases, J. Chromatogr. A. 1217 (2010) 814–856. https://doi.org/10.1016/j.chroma.2009.10.022.
[33] M. Ferri, S. Baürer, B. Alshaar, M. Wolter, T. Ikegami, C. West, M. Lämmerhofer, Fragment-based design of zwitterionic, strong cation- and weak anion-exchange type mixed-mode liquid chromatography ligands and their chromatographic exploration, Submitt. Publ. J Chromatogr A. (2019).
[34] C. West, Y. Zhang, L. Morin-Allory, Insights into chiral recognition mechanisms in supercritical fluid chromatography. I. Non-enantiospecific interactions contributing to the retention on tris-(3,5-dimethylphenylcarbamate) amylose and cellulose stationary phases, J. Chromatogr. A. 1218 (2011) 2019–2032. https://doi.org/10.1016/j.chroma.2010.11.084.
[35] C. West, G. Guenegou, Y. Zhang, L. Morin-Allory, Insights into chiral recognition mechanisms in supercritical fluid chromatography. II. Factors contributing to enantiomer separation on tris-(3,5-dimethylphenylcarbamate) of amylose and cellulose stationary phases, J. Chromatogr. A. 1218 (2011) 2033–2057. https://doi.org/10.1016/j.chroma.2010.11.085.
[36] R.-I. Chirita, C. West, S. Zubrzycki, A.-L. Finaru, C. Elfakir, Investigations on the chromatographic behaviour of zwitterionic stationary phases used in hydrophilic interaction chromatography, Hydrophilic Interact. Chromatogr. 1218 (2011) 5939–5963. https://doi.org/10.1016/j.chroma.2011.04.002.
[37] S. Khater, Y. Zhang, C. West, Insights into chiral recognition mechanism in supercritical fluid chromatography III. Non-halogenated polysaccharide stationary phases, J. Chromatogr. A. 1363 (2014) 278–293. https://doi.org/10.1016/j.chroma.2014.06.084.
[38] S. Khater, Y. Zhang, C. West, Insights into chiral recognition mechanism in supercritical fluid chromatography IV. Chlorinated polysaccharide stationary phases, J. Chromatogr. A. 1363 (2014) 294–310. https://doi.org/10.1016/j.chroma.2014.06.026.
[39] S. Khater, C. West, Characterization of three macrocyclic glycopeptide stationary phases in supercritical fluid chromatography, J. Chromatogr. A. 1604 (2019) 460485. https://doi.org/10.1016/j.chroma.2019.460485.
[40] S. Bäurer, M. Ferri, A. Carotti, S. Neubauer, R. Sardella, M. Lämmerhofer, Mixed-mode chromatography characteristics of chiralpak ZWIX(+) and ZWIX(−) and elucidation of their chromatographic orthogonality for LC × LC application, Anal. Chim. Acta. (2019) S0003267019311675. https://doi.org/10.1016/j.aca.2019.09.068.
[41] V. Mimini, F. Ianni, F. Marini, H. Hettegger, R. Sardella, W. Lindner, Electrostatic attraction-repulsion model with Cinchona alkaloid-based zwitterionic chiral stationary phases exemplified for zwitterionic analytes, Anal. Chim. Acta. 1078 (2019) 212–220. https://doi.org/10.1016/j.aca.2019.06.006.
[42] C. West, E. Lesellier, Characterisation of stationary phases in subcritical fluid chromatography with the solvation parameter model: III. Polar stationary phases, J. Chromatogr. A. 1110 (2006) 200–213. https://doi.org/10.1016/j.chroma.2006.01.109.
[43] C. West, E. Lesellier, Characterisation of stationary phases in subcritical fluid chromatography by the solvation parameter model: II. Comparison tools, J. Chromatogr. A. 1110 (2006) 191–199. https://doi.org/10.1016/j.chroma.2006.02.002.

Figure captions

Figure 1. Structures of the chiral selectors in the 11 stationary phases compared.

Figure 2. Hierarchical cluster analysis on the normalized retention data (normalized log k values) measured for the 161 analytes in Table S1 on the 11 stationary phases in Figure 1. Retention dissimilarity in the abscissa reflects Euclidean distance between the stationary phases. Chromatographic conditions: CO_2-methanol 90:10 (v/v), 25°C, 15 MPa, 3 mL/min.

Figure 3. Coefficients of the normalized LSER models calculated with Equation (1) and the retention data measured for the 161 achiral analytes in Table S1 for the eleven stationary phases described in Figure 1. Chromatographic conditions: CO_2-methanol 90:10 (v/v), 25°C, 15 MPa, 3 mL/min.

Figure 4. Plots of logarithms of retention factors for the analytes in Table S1 on the Chiralpak **ZWIX** columns compared to (a) an anion-exchange stationary phase (Chiralpak **QN-AX**) and (b) a cation-exchange stationary phase (the in-house prepared **SCXSS**). Black diamonds are hydrophobic analytes, open circles are polar non-ionizable analytes, red triangles are acidic compounds bearing a negative charge, blue squares are basic compounds bearing a positive charge. The interrupted line is the first bisector indicating identical retention values. The continuous grey line in (b) is showing the trend line between hydrophobic analytes. Chromatographic conditions: CO_2-methanol 90:10 (v/v), 25°C, 15 MPa, 3 mL/min.

Figure 5. Spider diagram based on the LSER models in Table 1 to observe the overall selectivity of the eleven columns in Figure 1. The 36 numbered columns are identified in Table S3. Chromatographic conditions: CO_2-methanol 90:10 (v/v), 25°C, 15 MPa, 3 mL/min.

Figure 6. Selected discriminant analyses between (a) early-eluting and late-eluting racemates, (b) early eluting separated and non-separated racemates and (c) late-eluting separated and non-separated racemates. Conditions: Chiralpak ZWIX(-),CO_2-methanol 90:10 (v/v), 25°C, 15 MPa, 3 mL/min, 58 racemates in Table S2. Negative features are common to the analytes in the left group; positive features are common to the analytes in the right group; zero features are non-discriminant.

Figure 7. Molecular modelling of the ligands and superimposition of them for useful comparison.

Figure 8. Chromatograms of (a) 5-Methyl-5-phenylhydantoin and (b) Alanine. Analytical conditions: Chiralpak ZWIX(+) (blue), Chiralpak QN-AX (red), QN (orange), QCISS (light green), QCITAU (dark green), SCXSS (black). Conditions (a) CO_2-MeOH 90:10 (v/v), 25 °C, 150 bar, 3 mL/min, UV detection (210nm); (b) gradient elution from 10% to 100% co-solvent (methanol containing 50 mM of ammonium formate and 5 % water), 25 °C, 150 bar, 0.5 mL/min, ESI(+)-MS detection m/z = 90.

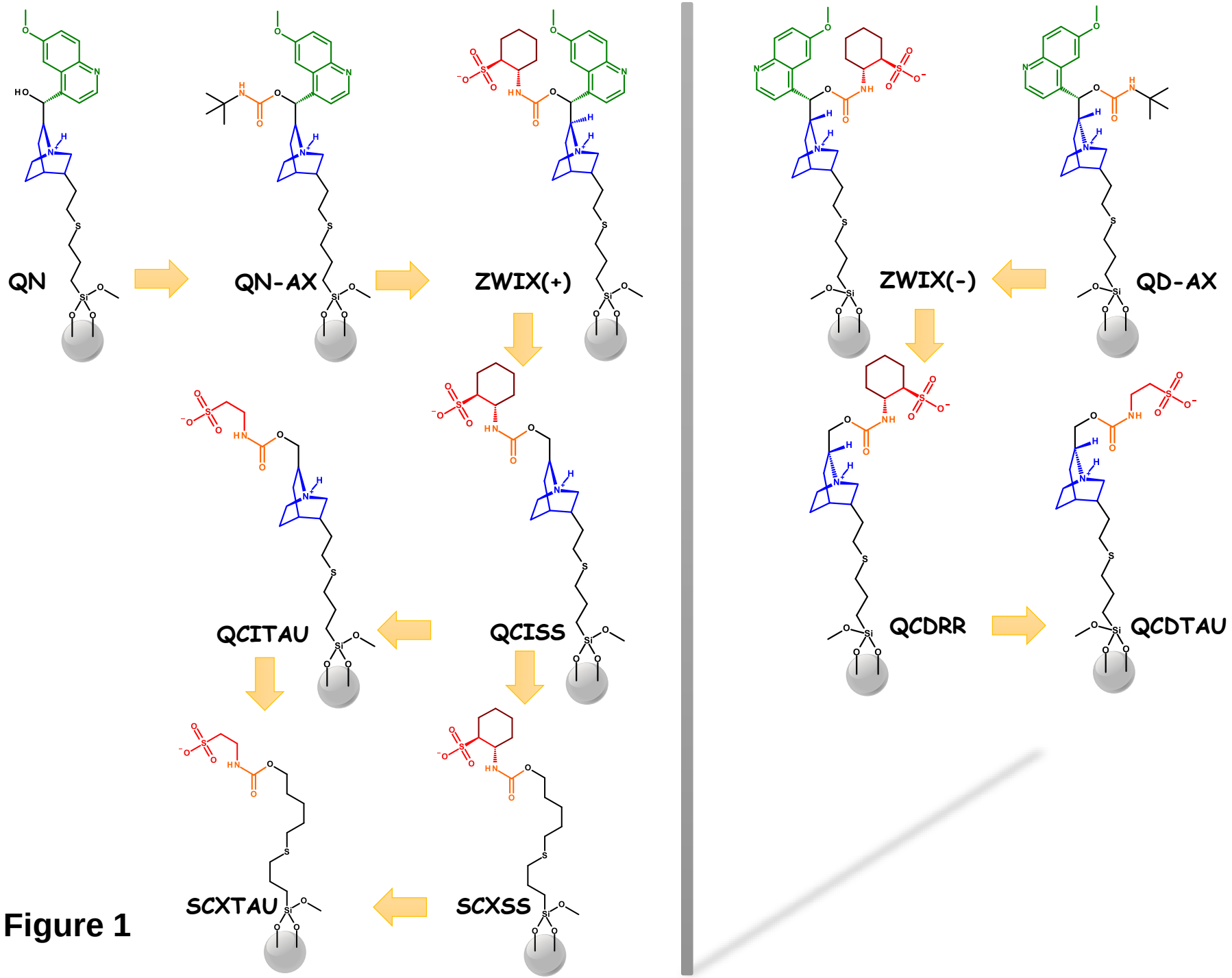
QN
QN-AX
ZWIX(+)
ZWIX(-)
QD-AX
QCITAU
QCISS
QCDRR
QCDTAU
SCXTAU
SCXSS

Figure 1

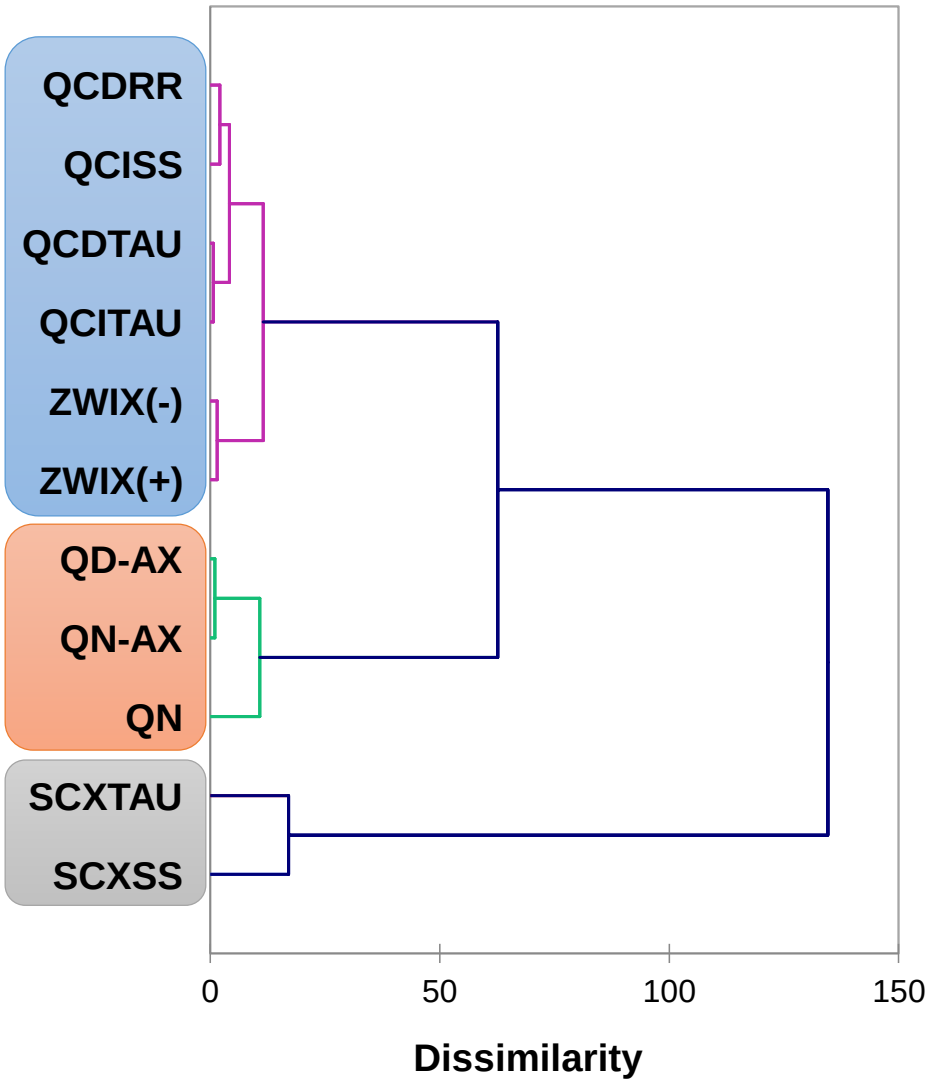
QCDRR
QCISS
QCDTAU
QCITAU
ZWIX(-)
ZWIX(+)
QD-AX
QN-AX
QN
SCXTAU
SCXSS
0
50
100
150
Dissimilarity

Figure 2

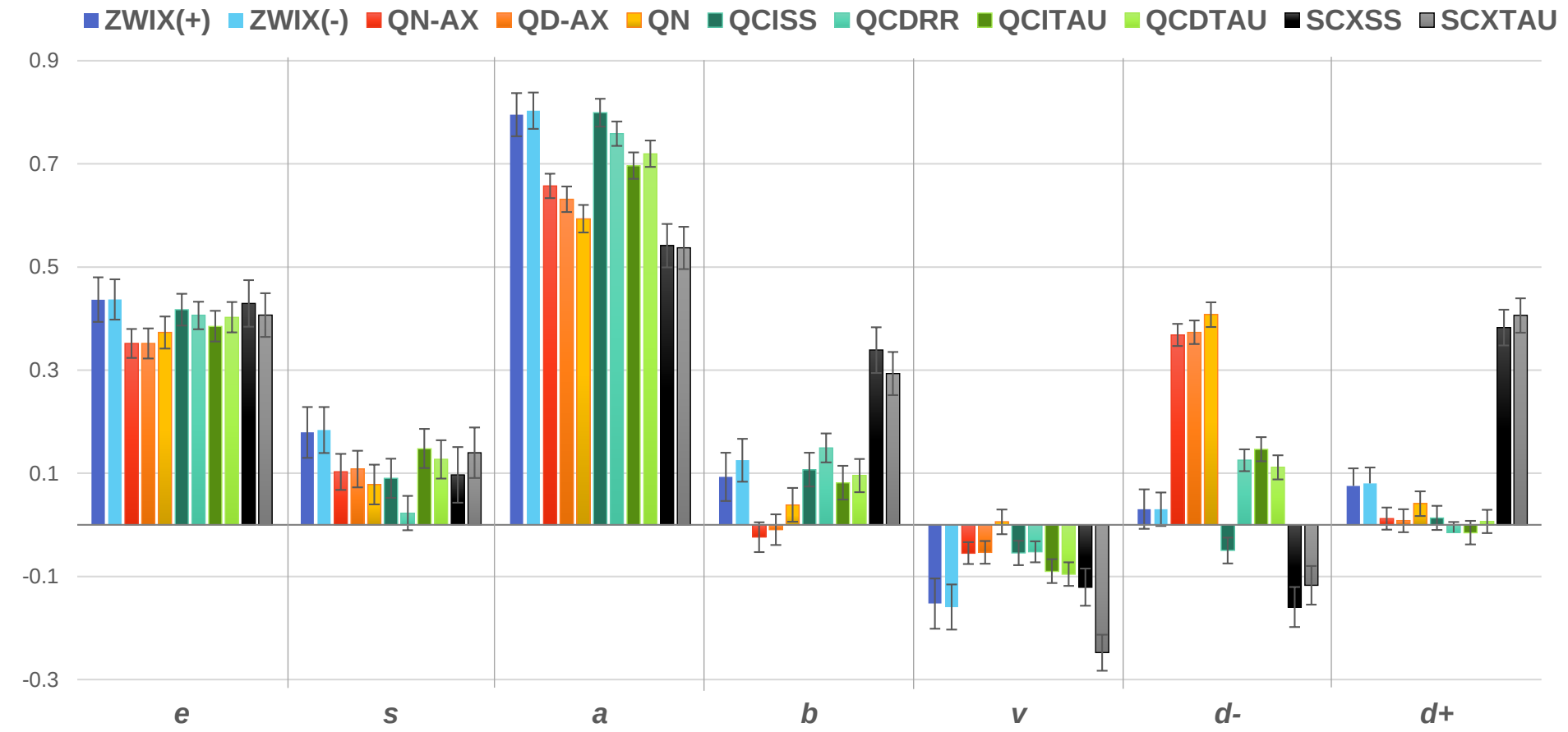
ZWIX(+)
ZWIX(-)
QN-AX
QD-AX
QN
QCISS
QCDRR
QCITAU
QCDTAU
SCXSS
SCXTAU
0.9
0.7
0.5
0.3
0.1
-0.1
-0.3
e
s
a
b
v
d-
d+

Figure 3

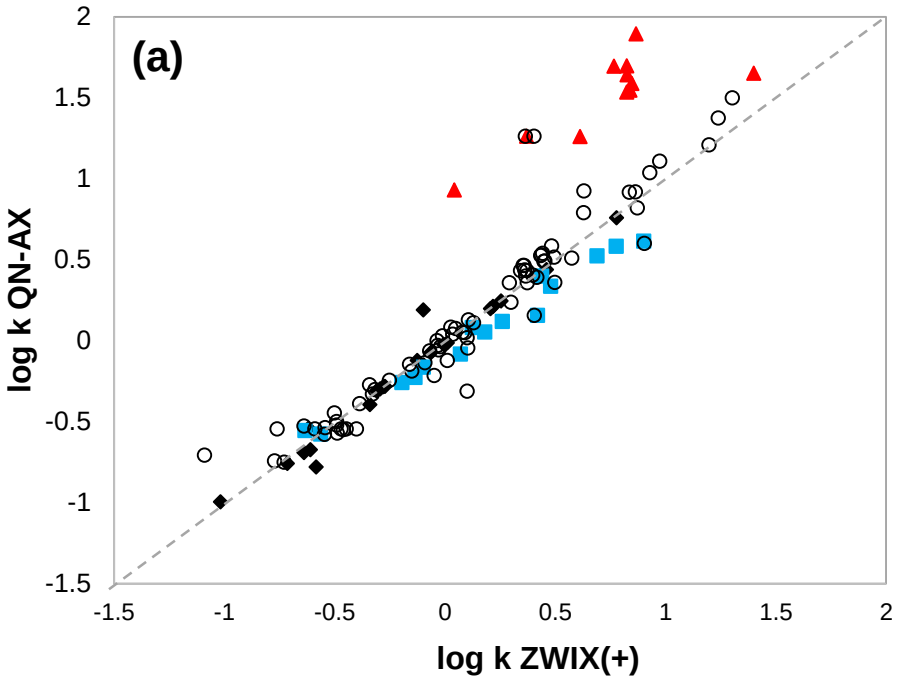
(a)
log k QN-AX
log k ZWIX(+)
2
1.5
1
0.5
0
-0.5
-1
-1.5
-1.5
-1
-0.5
0
0.5
1
1.5
2

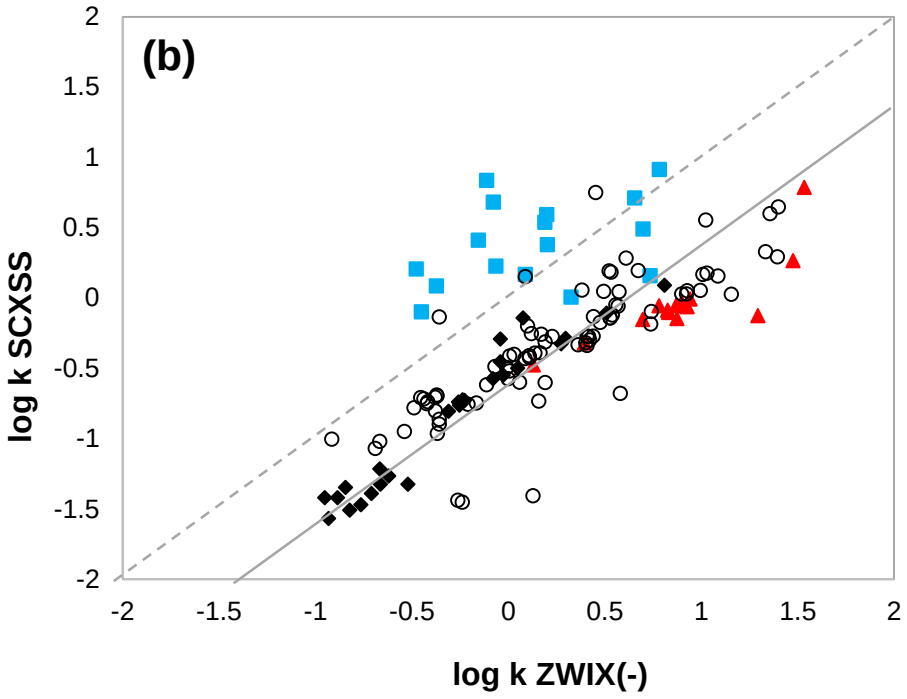
(b)
log k SCXSS
log k ZWIX(-)
2
1.5
1
0.5
0
-0.5
-1
-1.5
-2
-2
-1.5
-1
-0.5
0
0.5
1
1.5
2

Figure 4

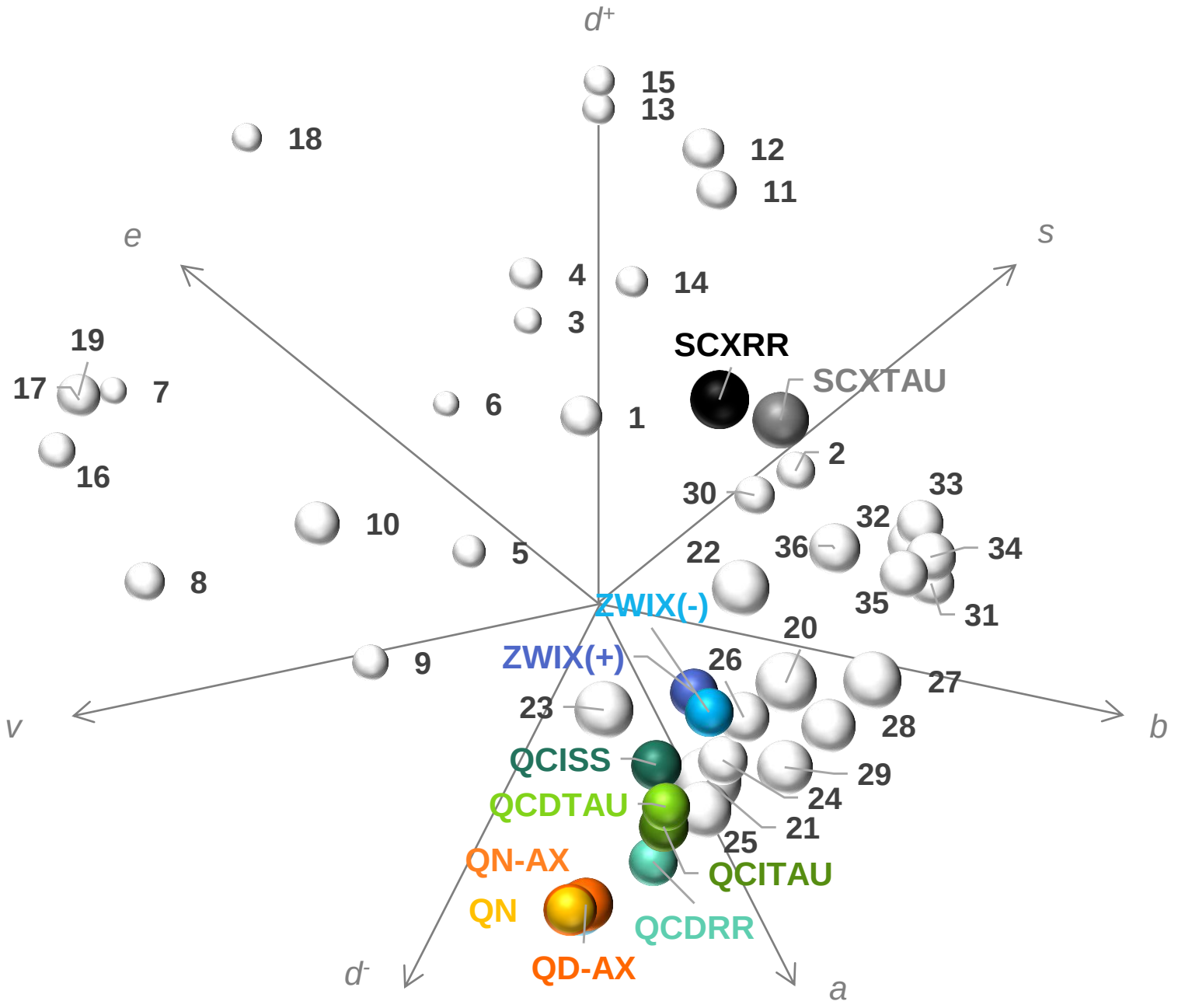
d+
15
13
18
12
11
e
s
4
14
3
19
SCXRR
17
7
6
1
SCXTAU
2
16
30
33
10
32
36
34
22
5
35
31
8
ZWIX(-)
20
9
ZWIX(+)
26
27
v
23
28
b
QCISS
29
QCDTAU
24
21
25
QN-AX
QCITAU
QN
QCDRR
d-
QD-AX
a

Figure 5

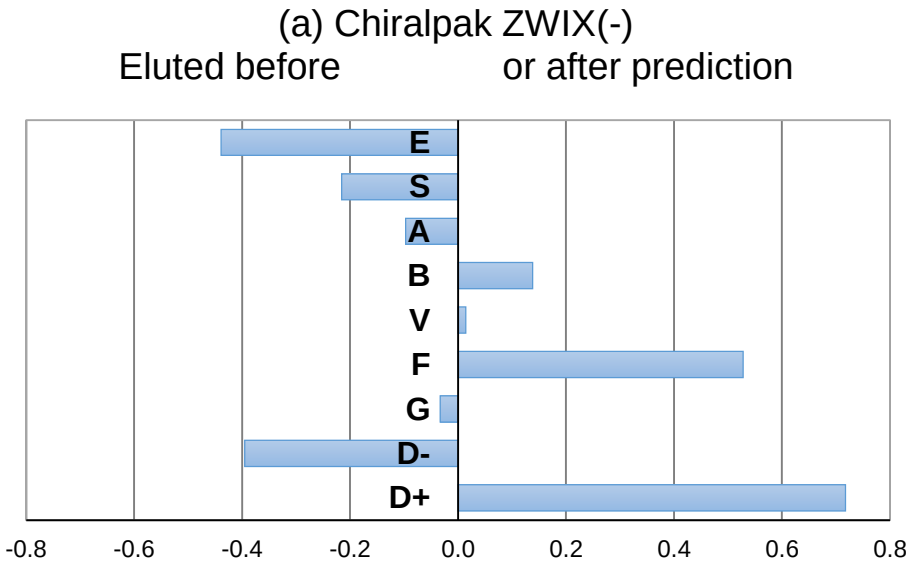
(a) Chiralpak ZWIX(-)
Eluted before
or after prediction
E
S
A
B
V
F
G
D-
D+
-0.8
-0.6
-0.4
-0.2
0.0
0.2
0.4
0.6
0.8

Figure 6

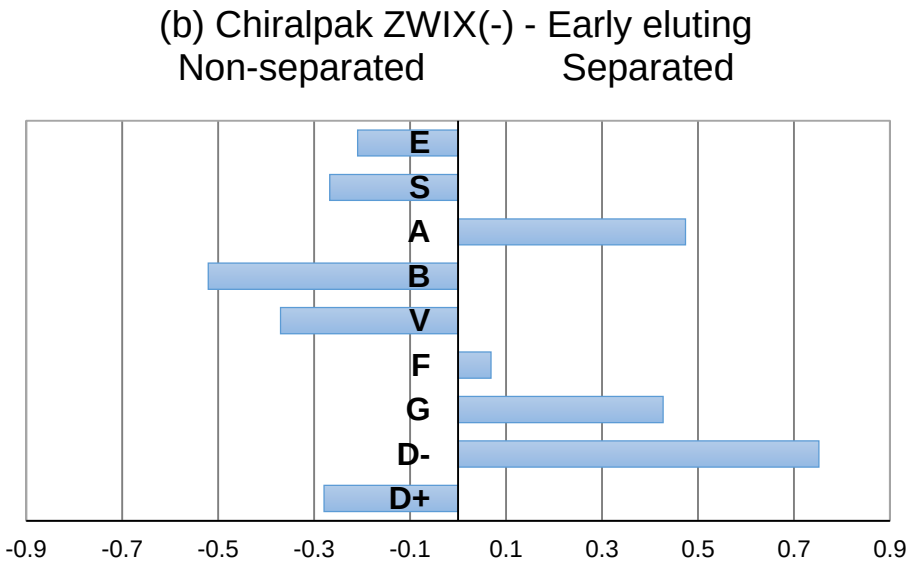

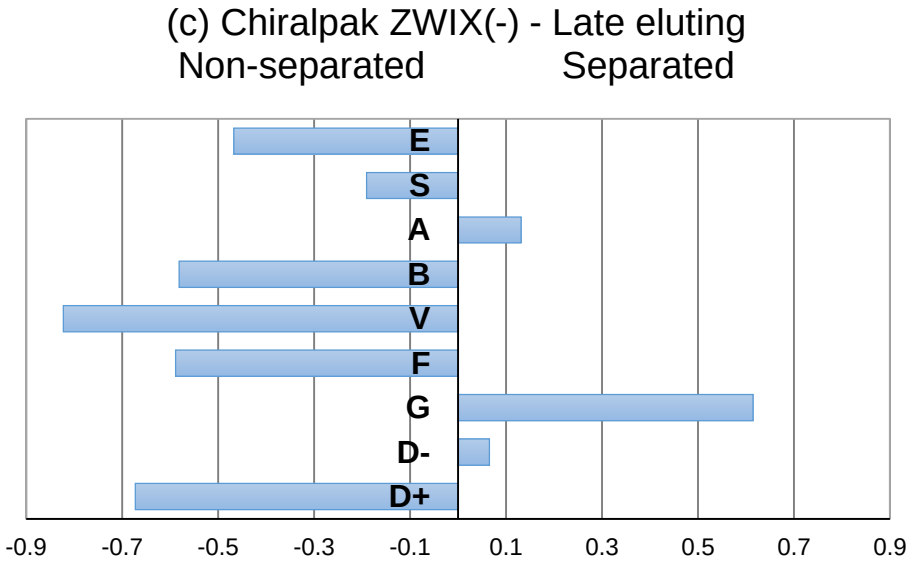

Figure 6 (continued)

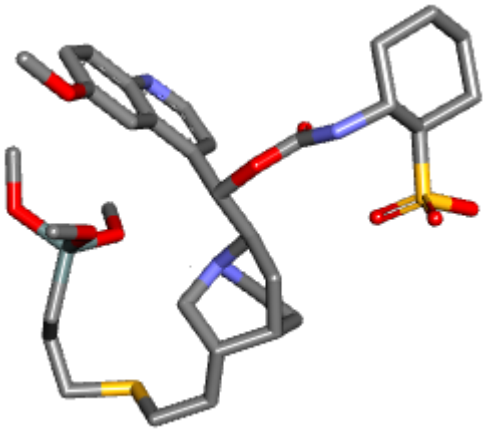

Chiralpak ZWIX(-)

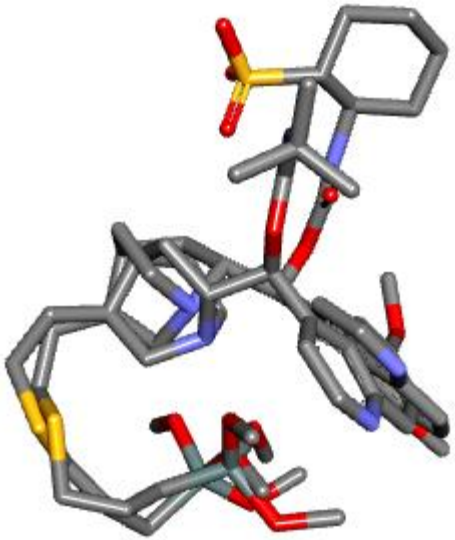

Chiralpak ZWIX(-) and QD-AX

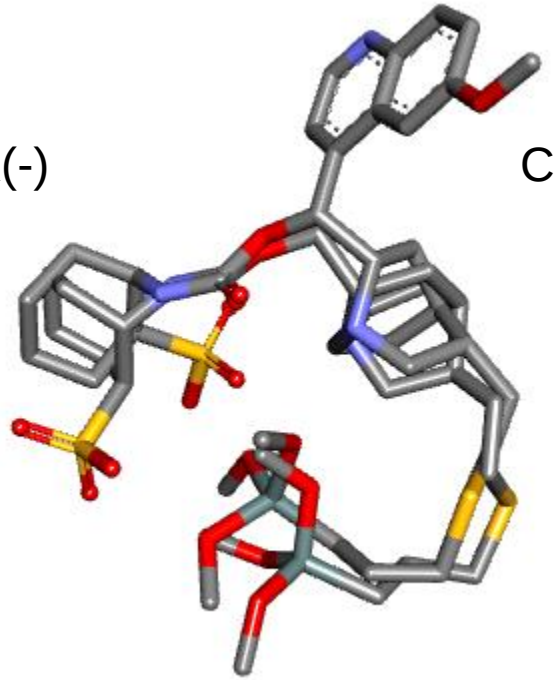

Chiralpak ZWIX(+) and QCISS

Figure 7

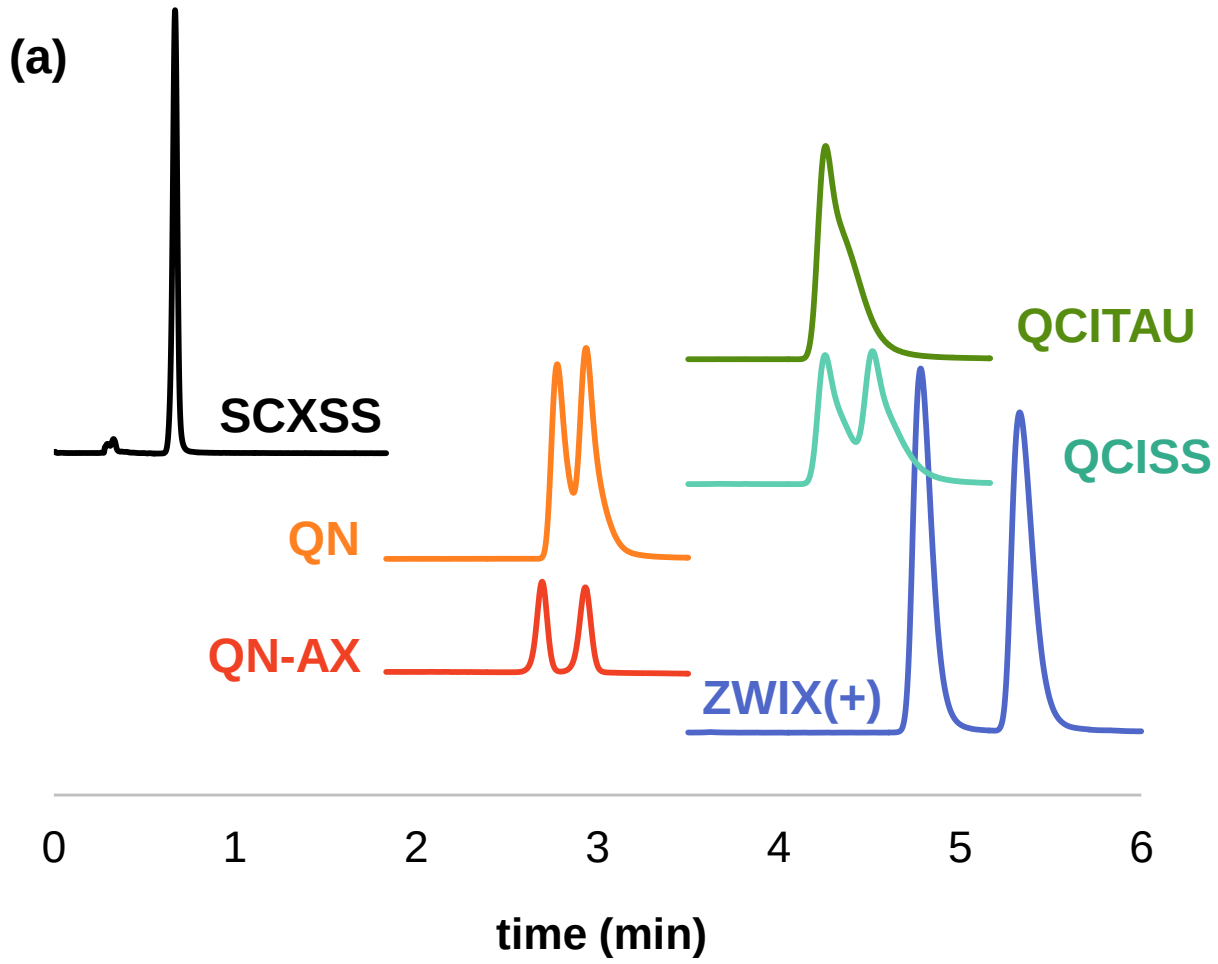

Figure 8

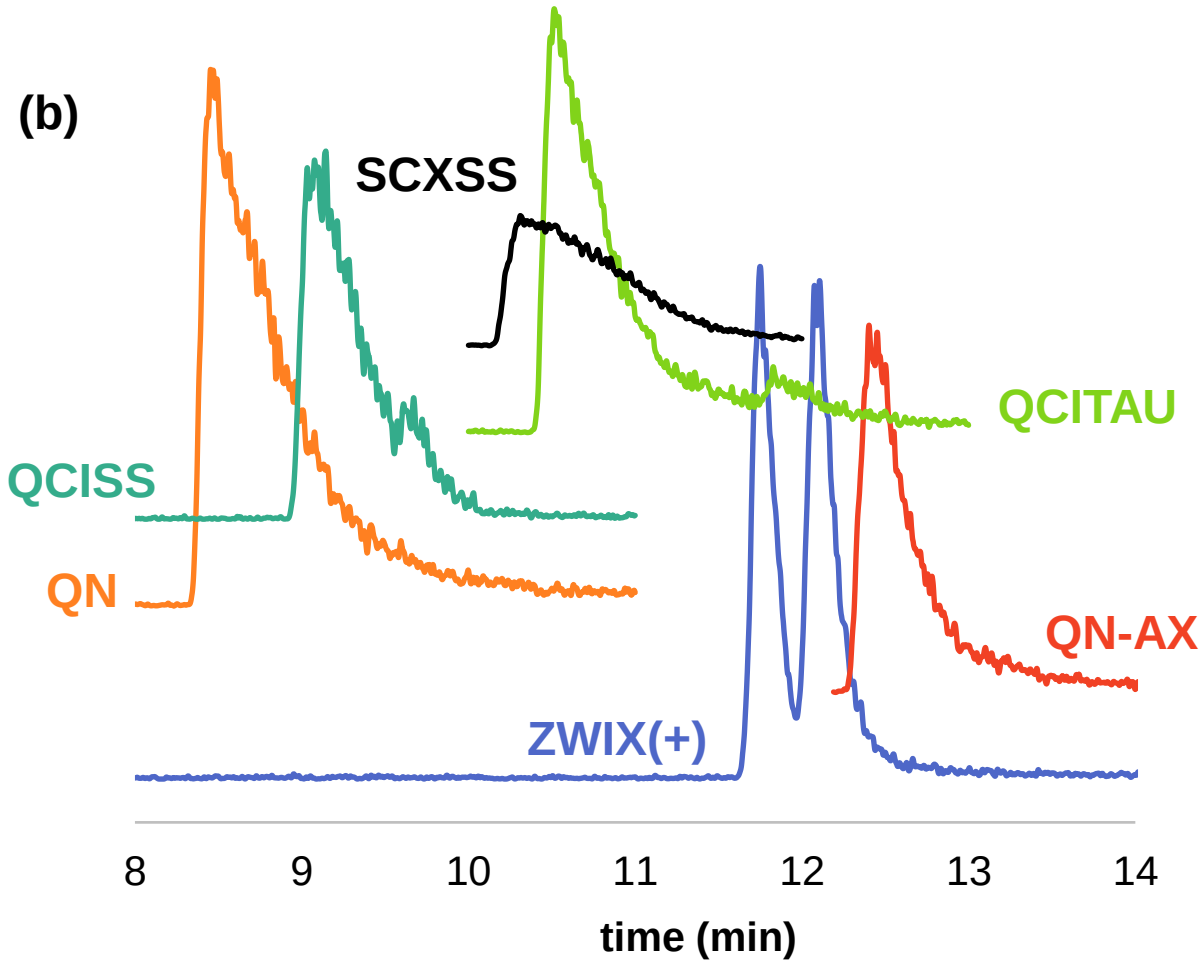

Figure 8

Table 1. system constants and statistics for the 11 columns tested
obtained with Eq.(2)
n is the number of solutes finally retained in the multiple linear regression;
R^2 is the determination coefficient; SE in the standard error in the estimate

Column	*c*	*e*	*s*	*a*	*b*	*v*	d^-	d^+	n	R^2_{adj}	*SE*
ZWIX(+)	-1.004	0.569	0.291	1.283	0.167	-0.241	0.046	0.190	126	0.876	0.190
	0.081	*0.056*	*0.080*	*0.067*	*0.084*	*0..077*	*0.058*	*0.086*			
ZWIX(-)	-0.916	0.537	0.283	1.333	0.217	-0.240	0.049	0.176	127	0.899	0.163
	0.068	*0.048*	*0.069*	*0.059*	*0.072*	*0.066*	*0.053*	*0.068*			
QN-AX	-0.916	0.493	0.179	1.477	-0.055	-0.093	1.154	0.036	145	0.944	0.153
	0.059	*0.039*	*0.060*	*0.054*	*0.067*	*0.036*	*0.067*	*0.063*			
QD-AX	-0.873	0.482	0.187	1.396	-0.022	-0.089	1.073	0.024	143	0.941	0.155
	0.061	*0.040*	*0.061*	*0.055*	*0.069*	*0.037*	*0.065*	*0.064*			
QN	-1.132	0.484	0.119	1.229	0.081	0.009	1.205	0.108	150	0.930	0.159
	0.058	*0.040*	*0.059*	*0.055*	*0.068*	*0.037*	*0.070*	*0.063*			
QCISS	-1.154	0.527	0.141	1.508	0.218	-0.082	-0.094	0.038	150	0.930	0.151
	0.058	*0.039*	*0.060*	*0.051*	*0.067*	*0.036*	*0.048*	*0.065*			
QCDRR	-0.842	0.481	0.034	1.359	0.297	-0.074	0.260	-0.039	147	0.949	0.122
	0.047	*0.032*	*0.049*	*0.042*	*0.056*	*0.029*	*0.044*	*0.053*			
QCITAU	-1.079	0.518	0.236	1.438	0.174	-0.142	0.309	-0.044	148	0.935	0.158
	0.058	*0.041*	*0.061*	*0.053*	*0.071*	*0.037*	*0.050*	*0.066*			
QCDTAU	-1.014	0.490	0.184	1.339	0.185	-0.137	0.212	0.018	147	0.939	0.139
	0.052	*0.036*	*0.054*	*0.047*	*0.062*	*0.033*	*0.044*	*0.058*			
SCXRR	-1.482	0.554	0.144	0.928	0.658	-0.191	-0.260	1.799	145	0.851	0.215
	0.093	*0.058*	*0.081*	*0.072*	*0.086*	*0.057*	*0.063*	*0.163*			
SCXTAU	-1.374	0.566	0.242	0.997	0.657	-0.446	-0.202	1.531	134	0.874	0.217
	0.103	*0.059*	*0.084*	*0.076*	*0.094*	*0.063*	*0.065*	*0.126*			

Table 2. Examples of enantioseparations for selected racemates on the ten chiral columns studied.

	ZWIX+	ZWIX-	QN-AX	QD-AX	QN	QCISS	QCDRR	QCITAU	QCDTAU	SCXSS
Oxazepam	×	×	✓	✓	✓	×	×	×	×	×
Mandelic acid, ethyl ester	✓	✓	✓	✓	×	✓	✓	✓	✓	×
5-methyl-5-phenylhydantoin	✓	✓	✓	✓	✓	✓	✓	×	×	×
Suprofen	✓	✓	✓	✓	×	×	×	×	×	×
Warfarin	✓	✓	✓	✓	×	×	×	×	×	×
Alanine	✓	✓	×	×	×	×	×	×	×	×
Glutamine	✓	✓	×	×	×	×	×	×	×	×